Contents lists available at ScienceDirect

Digital Chinese Medicine

journal homepage: http://www.keaipublishing.com/dcmed

Inhibition of photoreceptor apoptosis in mice with retinitis pigmentosa through NF-κB/NLRP3 pathway suppression with *Lycium barbarum* polysaccharide

WANG Ying[a], DENG Ying[b], LU Jing[c, d], PENG Jun[a, c], ZHOU Yasha[a, b, c], YANG Yijing[c*], PENG Qinghua[a*]

a. Department of Ophthalmology, The First Hospital of Hunan University of Chinese Medicine, Changsha, Hunan 410007, China

b. School of Traditional Chinese Medicine, Hunan University of Chinese Medicine, Changsha, Hunan 410208, China

c. Hunan Provincial Key Laboratory for the Prevention and Treatment of Ophthalmology and Otolaryngology Diseases with Chinese Medicine, Changsha, Hunan 410208, China

d. Medical School, Hunan University of Chinese Medicine, Changsha, Hunan 410208, China

ARTICLE INFO

Article history
Received 02 July 2023
Accepted 04 September 2023
Available online 25 September 2023

Keywords
Retinitis pigmentosa (RP)
Lycium barbarum polysaccharide (LBP)
Apoptosis
NF-κB/NLRP3 pathway
Oxidative stress

ABSTRACT

Objective To explore whether *Lycium barbarum* polysaccharide (LBP) can reduce the apoptosis of retinal photoreceptor cells in retinitis pigmentosa (RP) mice by inhibiting nuclear factor-kappa B (NF-κB)/NOD-like receptor thermal protein domain-associated protein 3 (NLRP3) signaling pathway.

Methods (i) *In vitro* experiments, mouse retinal ganglion cells (661W cells) were divided into normal, model, LBP low-dose (LBP-L, 40 mg/L), LBP middle-dose (LBP-M, 80 mg/L), LBP high-dose (LBP-H, 160 mg/L), and positive drug control (NLRP3 inhibitor, 160 mg/L) groups. And the 661W cells were exposed to varying concentrations of H_2O_2 ranging from 50 to 400 μmol/L to determine the optimal concentration for inducing apoptosis (200 μmol/L). Then the cell viability was assessed using Cell Counting Kit-8 (CCK-8), while the apoptosis rate was detected by flow cytometry; the expression of NLRP3 was detected by immunofluorescence; and the expression of apoptosis markers was detected by enzyme-linked immunosorbent assay (ELISA) and Western blot (WB). (ii) *In vivo* assays were carried out with the use of C57/BL6 and Rd10 mice. The animal experimental groups were divided into normal, model, LBP-L, LBP-M, LBP-H, and NLRP3 inhibitor groups, in which the normal group was C57/BL6 mice and the other groups were Rd10 mice. Ten mice were included in each group, and the corresponding drugs were administered intragastrically for a duration of four weeks. NF-κB/NLRP3 pathway and the expression of apoptosis markers were observed by electroretinogram, histopathological examination, and WB to assess the effects of LBP on retinal photoreceptor cell apoptosis.

Results (i) *In vitro* experiments, compared with the normal group, the apoptosis rate of 661W cells in model group was significantly increased ($P < 0.01$), and the expression levels of key proteins of NF-κB/NLRP pathway, such as NLRP3, NF-κB, p-NF-κB, and pro-apoptotic protein caspase-3, were up-regulated ($P < 0.01$). The rate of Bax/Bcl-2 was increased ($P < 0.01$), and the concentrations of interleukin (IL)-1β and tumor necrosis factor (TNF)-α were significantly increased ($P < 0.01$). Compared with the model group, high dose of LBP decreased the apoptosis rate of 661W cells ($P < 0.01$), and down-regulated the expression levels

*Corresponding author: PENG Qinghua, E-mail: pqh410007@126.com. YANG Yijing, E-mail: 292698530@qq.com.

Peer review under the responsibility of Hunan University of Chinese Medicine.

DOI: 10.1016/j.dcmed.2023.10.006

Citation: WANG Y, DENG Y, LU J, et al. Inhibition of photoreceptor apoptosis in mice with retinitis pigmentosa through NF-κB/NLRP3 pathway suppression with *Lycium barbarum* polysaccharide. Digital Chinese Medicine, 2023, 6(3): 307-316.

of the key proteins of NF-κB/NLRP3 pathway, including NF-κB, NLRP3, p-NF-κB, and caspase-3 ($P < 0.01$). The rate of Bax/Bcl-2 was decreased ($P < 0.01$), and the concentrations of IL-1β and TNF-α were decreased ($P < 0.01$). (ii) *In vivo* experiments, high dose of LBP significantly increased morphological changes in the outer nuclear layer (ONL) thickness of Rd10 mice, as well as functional changes in the amplitudes of the a-wave and b-wave ($P < 0.01$), which also down-regulated the expression levels of NF-κB ($P < 0.05$), NLRP3, p-NF-κB, and caspase-3 ($P < 0.01$), reduced the Bax/Bcl-2 rate ($P < 0.01$), and decreased the concentrations of IL-1β ($P < 0.01$) and TNF-α ($P < 0.05$).

Conclusion LBP could improve both retinal morphology and function, providing protection to photoreceptors from apoptosis through the inhibition of the NF-κB/NLRP3 pathway.

1 Introduction

Retinitis pigmentosa (RP) is a diverse group of ocular disorders characterized by the progressive degeneration of the retina, affecting approximately 1.5 million individuals worldwide [1]. Key clinical manifestations of RP include the gradual, progressive loss of visual field, bone spicule formation, and blood vessel constriction, ultimately culminating in vision impairment [2]. Currently, the underlying etiology of RP remains poorly elucidated, and regrettably, there is no known remedy. Genetic mutations are recognized as the primary trigger of photoreceptor cell loss and subsequent dysfunction of the retinal pigment epithelium (RPE) [3]. Reactive oxygen species (ROS) like hydrogen peroxide (H_2O_2), nitroxides, and peroxynitrite, which were generated during phototransduction, played a vital role in sustaining normal visual function [4]. The disruption of the equilibrium between ROS synthesis and anti-oxidant defenses resulted in oxidative damage in photoreceptors and RPE, further exacerbating the generation of excessive ROS [5]. It was reported that anti-oxidants, such as vitamin A, and the inhibition of apoptosis pathways linked to oxidative stress were associated with the prevention of photoreceptor degeneration [6-8]. Hypoxia and oxidative stress were reported to have up-regulated inflammatory cytokines, including tumor necrosis factor (TNF)-α, interleukin (IL)-1β, IL-17, and IL-18 in patients with RP [9]. Oxidative stress and ROS accumulation also affected the expression of microRNAs, which induced the release of inflammatory cytokines in RP mice [10, 11]. Studies also showed that photoreceptor apoptosis played a pivotal role in oxidative stress and inflammation in RP mice. What's more, the increase of ROS production could induce the inflammation in RPE cells, and it was demonstrated that inflammatory processes involving nuclear factor-kappa B (NF-κB) and NOD-like receptor thermal protein domain-associated protein 3 (NLRP3), induced by ROS, were prominent features in RP [12, 13].

Gouqizi (*Lycium barbarum*) is a kind of traditional Chinese medicine with extensive use in China, renowned for its hepatoprotective and nephroprotective properties, as well as its ability to tonify essence and enhance eyesight. In the past two decades, researchers have identified more than 200 distinct bioactive components in Gouqizi (*Lycium barbarum*), encompassing polysaccharides, polyphenols, carotenoids, amino acids, and vitamins. At present, research on Gouqizi (*Lycium barbarum*) has entered a new stage. Pharmacological assessments and clinical medical experiments have yielded compelling findings, highlighting the unique nutritional and medicinal attributes of Gouqizi (*Lycium barbarum*), which include its liver and eye-nourishing properties, its capacity to replenish Yin and support kidney health, regulation of blood sugar levels, as well as its potential for anti-cancer, anti-aging, and anti-oxidant effects [14]. Gouqizi (*Lycium barbarum*) can treat various diseases, including visual impairment, aging-related issues, infertility, and fatigue. *Lycium barbarum* polysaccharide (LBP) is the water-soluble protein polysaccharide extracted and isolated from the *Lycium barbarum* plant, which is valuable bioactive component with anti-oxidant, anti-inflammatory, anti-apoptotic, and neuroprotective properties [15]. Studies showed that LBP treatment down-regulated NF-κB and NLRP3 expression levels, offering protection against cellular injury [16, 17]. In this study, we investigated the anti-apoptosis effect of LBP on photoreceptor apoptosis via the suppression of NF-κB/NLRP3 pathway.

2 Materials and methods

2.1 Reagents

Reagents utilized in the study were as follows. LBP powder of 50% purity (Beijing Solarbio life sciences, China), hematoxylin and eosin (HE) staining kit (Beyotime Biotechnology, China), Annexin V-APC Reagent E-CK-A117 (Elabscience, China), Cell Counting Kit-8 (CCK-8) (Topscience, America), methylene bis acrylamide (Sigma, America), tris (Sigma, America), glycine (Sigma, America), diethyl pyrocarbonate (Sigma, America), Dulbecco Modified Eagle Medium and Ham F12 (DMEM/F12) (Sigma, America), nonfat milk (Applygen

Technologies, America), protease inhibitor (Applygen Technologies, America), protein phosphatase inhibitor (Applygen Technologies, America), 6X sample buffer (Cowin Bio, China), mouse IL-1β enzyme-linked immunosorbent assay (ELISA) kit (YanKang Bio, China), mouse TNF-α ELISA kit (Beyotime, China), NF-κB antibody (CST, America), p-NF-κB (Ser536) antibody (Cell Signaling Technology, America), NLRP3 antibody (Abcam, UK), Bcl-2 (Beyotime, China), Bax antibody (Cell Signaling Technology, America), caspase-3 antibody (Abcam, UK), β-actin antibody (Proteintech, China), horseradish peroxidase (HRP) goat anti-mouse IgG and HRP goat anti-rabbit IgG (Proteintech, China), eyeball fixative (Powerful Biology, America), radio immunoprecipitation assay (RIPA) (Biyuntian Biotechnology, China), 1.25% tribromethanol (Hefei TNJ Chemical Industry, China), 0.5% tropicamide (Shentian Pharmaceutical Co., Ltd., China), and staining kit for histopathological determination (Beyotime Biotechnology, China).

2.2 Experimental equipments

The equipments employed in this study were as follows. OCT fundus photography all-in-one machine (Phoenix Research Labs, FPphoe-Micron-IV), Ganzfeld electroretinograph (Phoenix Research Labs, phoenix micron IV), embedding machine (Wuhan Junjie Electronic Co., Ltd., JB-P5), ophthalmic operating microscope (Hangzhou Liuliu Visual Medical equipment Co., Ltd., YZ20T4), pathological slicer (Shanghai Leica instrument Co., Ltd., RM2016), positive optical microscope (Nikon, Nikon Eclipse E100), imaging system (Nikon, Nikon DS-M3), fluorescence quantitative PCR instrument (Thermo, PIKOREAL96), horizontal agarose electrophoresis tank (Liuyi, DYCP-31DN), magnetic stirrer (Thunder magnetic, JB-13), freezing table (Wuhan Junjie Electronic Co., Ltd., JB-L5), automated enzyme labeling instrument (Biotek instruments, Inc, 800Ts), Leica DM4 B fluorescence microscope (Leica Microsystems (Shanghai) Co., Ltd., DM4B), ECL luminescent instrument (Thermo Fisher Scientific, iBright CL750), and Leica DCM8 microscope [Leica Microsystems (Shanghai) Co., Ltd., Leica DCM8].

2.3 LBP solution preparation

After dissolving the LBP powder in distilled water to achieve a concentration of 160 mg/L, the sample was filtered using a 40 μm microporous polyvinylidene fluoride (PVDF) membrane. The LBP solution with a concentration of 160 mg/L was diluted to 40 mg/L and 80 mg/L.

2.4 Culture and treatment of the 661W cells

The 661W cells (mouse retinal photoreceptor cells) (obtained from Yaji Biotechnology, China) were cultured in a 1 : 1 mixture of DMEM/F12, supplemented with 100 U/mL penicillin and 0.1 mg/mL streptomycin, and maintained at 37 °C in an environment with 5% CO_2. The 661W cells were treated with H_2O_2 of 50, 100, 200, and 400 μmol/L, respectively, and the cell ability was detected by CCK-8 to select the best H_2O_2 concentration (200 μmol/L) [5]. The cells were categorized into six groups: the normal group, with cells treated with regular culture medium only; the model group, with cells exposed to H_2O_2 in regular culture medium for 24 h; the LBP low-dose (LBP-L), LBP middle-dose (LBP-M), and LBP high-dose (LBP-H) groups, with cells exposed to H_2O_2 in regular culture medium for 24 h, the LBP-L, LBP-M, and LBP-H, with cells exposed to H_2O_2 (along with 50 μL of LBP solution of different concentrations); and the NLRP3 inhibitor (Muscone) group, with cells exposed to H_2O_2 with 50 μL of Muscone (160 mg/L) [18]. Each group consisted of five samples.

2.5 Cell apoptosis assessment

After being treated for 24 h, the cells were collected and resuspended in 1 mL phosphate-buffered saline (PBS), and then incubated at 37 °C for 30 min with CM-H2DCF-DA at a concentration of 1 mmol/L to assess cell apoptosis rates in live cells using flow cytometry.

2.6 CCK-8 assay

661W cells in logarithmic growth were inoculated in a 96-well plate for adherence with 1 000 cells per well. After intervention for 48 h, each well was added with 100 μL of CCK-8 working solution and placed in an incubator for 1.5 h. The absorbance at 450 nm was measured using an automated enzyme labeling instrument for the calculation of relative proliferation rate.

2.7 ELISA for 661W cells

50 μL of standard solutions at varying concentrations were designated into the wells. Initially, the testing sample (10 μL) was mixed with a sample diluent (40 μL), and then added to the sample wells. Blank wells were exempted from this treatment. Subsequently, 100 μL of HRP-labeled antibody was added into standard wells and sample wells, which were sealed with films for reaction. The wells were later incubated in water bath at 37 °C for 60 min. Following this, the liquid was discarded. The wells were then gently blotted on absorbent paper and washed with the washing solution for 1 min. After that, the washing solution was discarded from the wells, which were blotted again on absorbent paper. This washing process was repeated five times. After being washed, the wells were added with 50 μL substrate, H_2O_2, and 3,3,5,5-tetramethylbenzidine (TMB), respectively, and incubated in darkness at 37 °C for 15 min. Following incubation,

50 μL of stop solution was added to sample wells and blank wells, whose optical density (OD) values were measured at 450 nm within a 15 min window.

2.8 Immunofluorescence

The treated 661W cells in section 2.4 were initially fixed with 4% paraformaldehyde (PFA) for 30 min at room temperature, washed twice with PBS for 3 min each time, and then permeabilized with 0.1% surface active agent Trition X-100 for 2 min at room temperature. Then, 30 μL of diluted NLRP3 (1 : 100) antibody was added and incubated for 30 min, followed by washing three times with PBS for 3 min each time. The secondary antibodies were treated in a similar manner. Finally, 10 μL of embedding solution was added. After 30 min, Leica DM4 B fluorescence microscope was utilized for imaging.

2.9 Western blot (WB) for the determination of protein expressions *in vitro*

The treated 661W cells in section 2.4 were lysed using chilled RIPA buffer. After centrifuging the lysate at 12 000 × g for 10 min at 4 °C, the supernatant was mixed with 30 μL of loading buffer and then boiled at 100 °C for 5 min. Subsequently, protein separation was achieved with the use of 15% sodium dodecyl sulphate-polyacrylamide gel electrophoresis (SDS-PAGE), followed by transferring onto a PVDF membrane. After blocking the membrane with 5% skimmed milk in PBS for 2 h, sequential incubations were conducted with primary antibodies overnight at 4 °C, and washed with PBS three times for 10 min each time, then the secondary antibodies were added and incubated at room temperature for 90 min, and washed with PBS three times for 10 min each time. Finally, images were exposed and captured using the ECL luminescent instrument. The primary antibodies used included mouse anti-NF-κB (1 : 1 000), anti-NLRP3 (1 : 1 000), anti-Bcl-2 (1 : 2 000), anti-Bax (1 : 2 000), and anti-caspase-3 (1 : 5 000), while the secondary antibodies comprised HRP-goat anti-mouse IgG (1 : 5 000), and HRP-goat anti-rabbit IgG (1 : 6 000). Quantity One was utilized for imaging quantitation.

2.10 Animals

The four-week-old RP model Rd10 mice (B6.CXB1-Pde6bRd10/J), were naturally mutated mice based on the C57/BL6 mice genetic background, sourced from the Jackson Laboratory (USA, 1911A11353). The C57/BL6 mice were obtained from and Hunan Slake Jingda Experimental Animal (China, ZS-202206280021). The laboratory animal license was SYXK (Xiang) 2019-0009. All mice were housed in a controlled environment at 22 ± 2 °C with a 12 h photoperiod. Experimental procedures involving animals were conducted in accordance with the guidelines and regulations established by the Animal Ethics Committee of Hunan University of Chinese Medicine (Approval No. LL2021042605).

Fifty Rd10 mice were randomized into five groups: model (no treatment), NLRP3 inhibitor (0.08 g/d administered intragastrically using Muscone), LBP-L (0.08 g/d intragastrically), LBP-M (0.16 g/d intragastrically), and LBP-H (0.32 g/d intragastrically) groups. The drugs were prepared by dissolving them in distilled water for later use, with a dose of 0.2 mL per gavage. Ten C57/BL6 mice were served as normal controls and received no treatment.

2.11 Electroretinogram (ERG)

Mice were anesthetized using 1.25% tribromethanol (intraperitoneal injection, the dose was 0.2 mL/10 g body weight), and were treated with 0.5% tropicamide (eye drops, one drop at a time) for mydriasis before oral administration of LBP. ERG was conducted using the Micron IV system.

2.12 Histopathologic evaluation of retinal tissue

The animals were euthanized, and their enucleated eyeballs were fixed using eyeball fixative. Subsequently, the fixed samples underwent a series of processes, encompassing dehydration, paraffin embedding, and sectioning. HE staining was performed with the use of the staining kit for histopathological determination according to manufacturer's instructions. Images were captured using a Leica DCM8 microscope.

2.13 ELISA for mice retinas

Retinas were isolated from the enucleated eyeballs, rinsed with precooled PBS to remove any blood or impurities remaining on the surface, weighed, and cut into as small pieces as possible for full homogenization for ELISA, following the procedure outlined in the section 2.7.

2.14 WB for the determination of protein expressions *in vivo*

Retinas were treated as described in section 2.13, then WB was performed, as described in section 2.9.

2.15 Statistical analysis

SPSS 25.0 was employed for data analysis and the data were expressed as mean ± standard deviation (SD). Group-comparisons were performed using one-way analysis of variance (ANOVA), with statistical significance set at $P < 0.05$. Graphs were generated using GraphPad Prism 9.5.

3 Results

3.1 Cell viability

Induction with H_2O_2 caused oxidative damage to 661W cells, with doses of 200 and 400 μmol/L H_2O_2 significantly affecting cell viability ($P < 0.01$). However, no discernible differences were observed between control cells and those exposed to 50 or 100 μmol/L H_2O_2 ($P > 0.05$). In subsequent experiments, considering that a concentration of 400 μmol/L H_2O_2 reduced the cell survival rate by more than half, which would increase the difficulty of later experiments. Therefore, 200 μmol/L H_2O_2 was selected to induce oxidative stress in 661W cells, as depicted in Figure 1A. To assess the effects of various concentrations of LBP on cell viability of 661W cells, the CCK-8 assay was employed. The results demonstrated that 160 mg/L of LBP exhibited the most substantial effects in restoring viability of 661W cells ($P < 0.01$), as shown in Figure 1B.

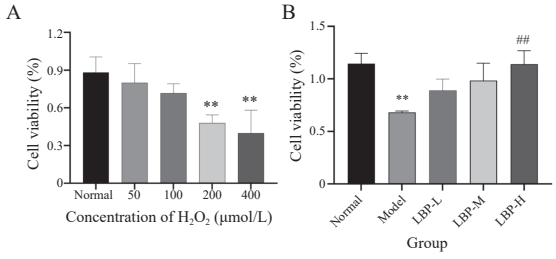

Figure 1 The cell viability of 661W cells
A, cell viability of 661W cells at different H_2O_2 concentrations. B, cell viability of 661W cells at different LBP concentrations. Data were expressed as mean ± SD. $^{**}P < 0.01$, compared with the normal group. $^{\#\#}P < 0.01$, compared with the model group.

3.2 Apoptosis inhibition in 661W cells following LBP treatment under oxidative stress

NLRP3 inhibitor could inhibit NF-κB/NLRP3 pathway and reduce apoptosis. Flow cytometry analysis revealed a significant increase ($P < 0.01$) in the apoptotic rate of 661W cells induced by H_2O_2 (200 μmol/L) (Figure 2). LBP-H treatment exhibited a remarkable inhibitory effect on cell apoptosis ($P < 0.01$), with a dose-dependent reduction in apoptosis as LBP concentration increased from low to high.

3.3 Down-regulation of IL-1β and TNF-α levels in 661W cells following LBP treatment under oxidative stress

The levels of IL-1β and TNF-α were measured using ELISA. The expression levels of IL-1β and TNF-α in 661W cells were significantly higher than those in normal group under oxidative stress ($P < 0.01$). However, the administration of LBP high dose reduced the expression of IL-1β and TNF-α in 661W cells under oxidative stress, which had a similar inhibitory effect to NLRP3 inhibitor ($P < 0.01$), as depicted in Figure 3.

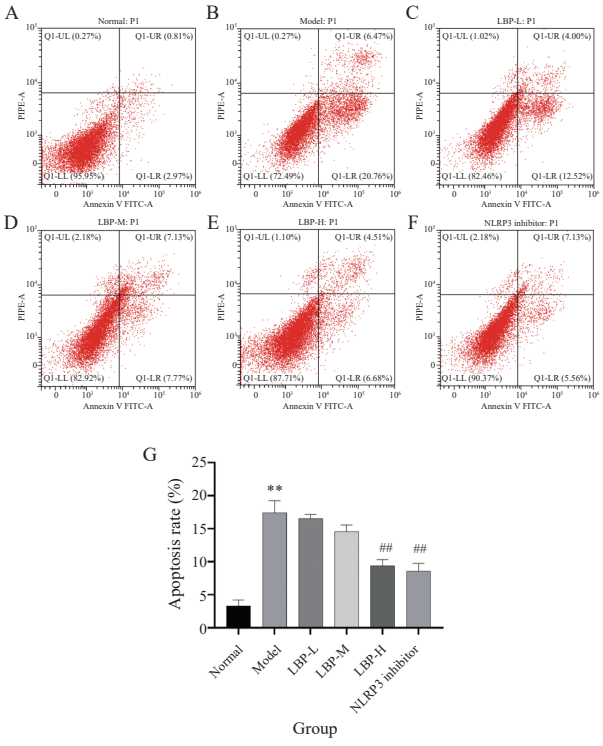

Figure 2 Apoptosis inhibition by LBP treatment under oxidative stress in 661W cells
A - F, the flow cytometry in the normal, model, LBP-L, LBP-M, LBP-H, and NLRP3 inhibitor groups, respectively. G, the apoptosis rate in each group. Data were expressed as mean ± SD. $^{**}P < 0.01$, compared with the normal group. $^{\#\#}P < 0.01$, compared with the model group.

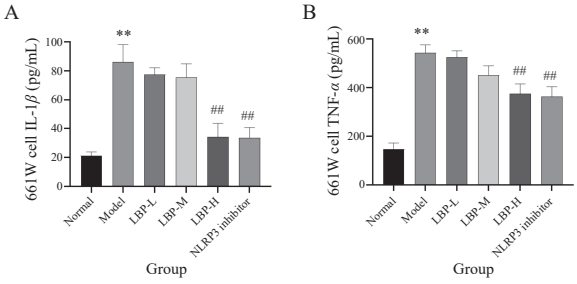

Figure 3 The expression levels of IL-1β and TNF-α in 661W cells by ELISA
A, the expression level of IL-1β. B, the expression level of TNF-α. Data were presented as mean ± SD. $^{**}P < 0.01$, compared with the normal group. $^{\#\#}P < 0.01$, compared with the model group.

3.4 Down-regulation of NLRP3 in 661W cells following LBP treatment under oxidative stress

NLRP3 protein expression level in 661W cells under oxidative stress was assessed via immunofluorescence (Figure 4).

The analysis of integrated OD revealed that H_2O_2 with the dose of 200 μmol/L resulted in an up-regulation of NLRP3 in 661W cells. However, the administration of LBP decreased NLRP3 protein expression, and this effect was similar to that observed with NLRP3 inhibitors ($P < 0.01$).

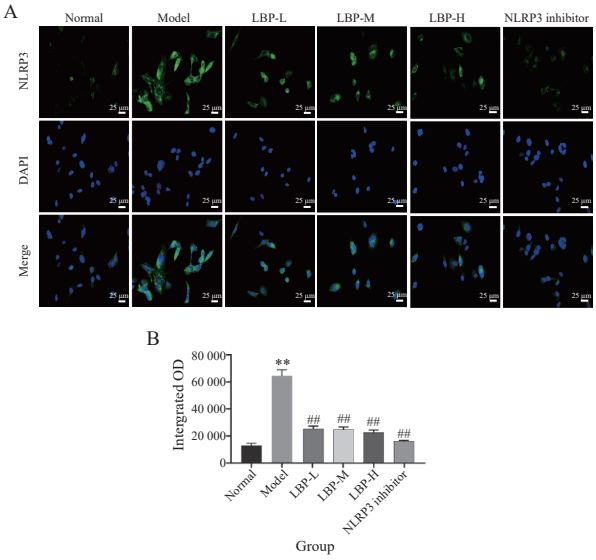

Figure 4 Down-regulation of NLRP3 level in 661W cells by LBP treatment under oxidative stress

A, immunofluorescence result of NLRP3 level in 661W cells. B, the intergrated OD of the immunofluorescence of the expression of NLRP3 in 661W cells. Data were expressed as mean ± SD. $^{**}P < 0.01$, compared with the normal group. $^{\#\#}P < 0.01$, compared with the model group.

3.5 Effects of LBP on protein expression *in vitro*

Precisely, in the model group, NF-κB, p-NF-κB, NLRP3, and caspase-3 protein levels were markedly elevated when compared with normal cells ($P < 0.01$), and the rate of Bax/Bcl-2 was up-regulated ($P < 0.01$). Moreover, in the LBP-H group, NF-κB, p-NF-κB, NLRP3, and caspase-3 expression, and the rate of Bax/Bcl-2 exhibited a marked reduction compared with the model group ($P < 0.01$). Notably, the inhibition of NLRP3 had the effect of diminishing the protein levels of NF-κB, p-NF-κB, NLRP3, caspase-3, and the rate of Bax/Bcl-2 in 661W cells under oxidative stress ($P < 0.01$). These results indicated that LBP effectively down-regulated NF-κB, p-NF-κB, and NLRP3 levels in 661W cells under oxidative stress, thereby providing protective effects against apoptotic events triggered by oxidative stress in these cells, as depicted in Figure 5.

3.6 LBP's effects on retinal function

ERG was performed to observe the retinal function across all groups, with a focus on obtaining a-wave (under dark adaptation, the action potentials of photoreceptor cells) and b-wave (under dark adaptation, the action potentials of photoreceptor cells, Müller cells, and bipolar cells) amplitudes. Notably, the a-wave and b-wave amplitudes displayed a significant decrease ($P < 0.01$) in Rd10 mice within the model group when compared with the normal group. However, following the administration of the high dose of LBP, there was a noteworthy increase in a-wave and b-wave amplitudes when compared with the model group ($P < 0.01$) (Figure 6). The results suggested that LBP had a protective effect on retinal function.

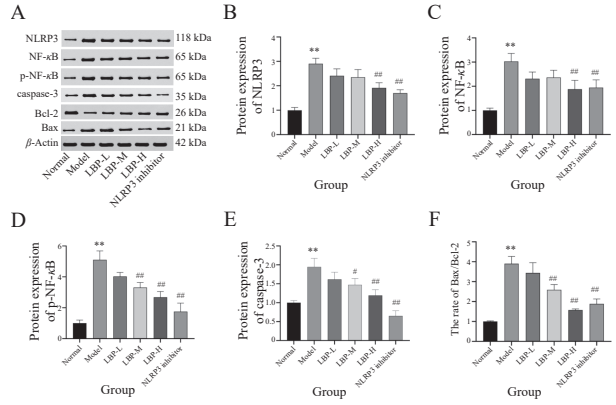

Figure 5 The expression levels of key proteins in NF-κB/NLRP3 pathway and apoptosis markers in different 661W cell groups

A, the protein bands of NLRP3, NF-κB, p-NF-κB, caspase-3, Bcl-2, and Bax in 661W cells. B - F, the quantitative evaluation of the proteins of NLRP3, NF-κB, p-NF-κB, caspase-3, and the rate of Bax/Bcl-2 in 661W cells, respectively. Data were expressed as mean ± SD. $^{**}P < 0.01$, compared with the normal group. $^{\#}P < 0.05$ and $^{\#\#}P < 0.01$, compared with the model group.

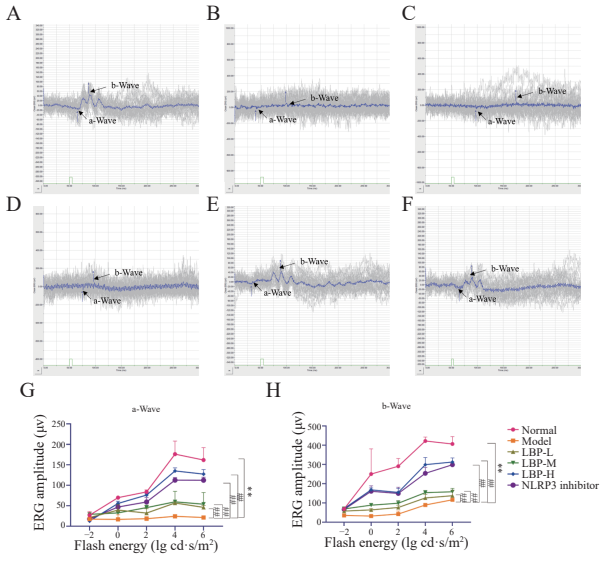

Figure 6 Retina function examined by ERG

A - F, ERG responses in the normal, model, LBP-L, LBP-M, LBP-H, and the NLRP3 inhibitor groups, respectively. G and H, a-wave and b-wave amplitudes in each group, respectively. Data were expressed as mean ± SD. $^{**}P < 0.01$, compared with the normal group. $^{\#\#}P < 0.01$, compared with the model group.

3.7 Effects of LBP on retinal tissue morphology

The retinal tissue morphology was meticulously assessed through HE staining in all groups, with a specific recording on the thickness of the outer nuclear layer (ONL). In Rd10 mice from the model group, the retinal tissue exhibited pronounced structural disorganization and remarkable atrophy when compared with the normal group (P < 0.01). However, the administration of LBP-H increased the thickness of retina, and mitigated the observed atrophy. In the LBP-H group, ONL thickness was markedly increased compared with the model group (P < 0.01). These results underscored the protective role of LBP in safeguarding retinal tissue integrity and alleviating photoreceptor loss (Figure 7).

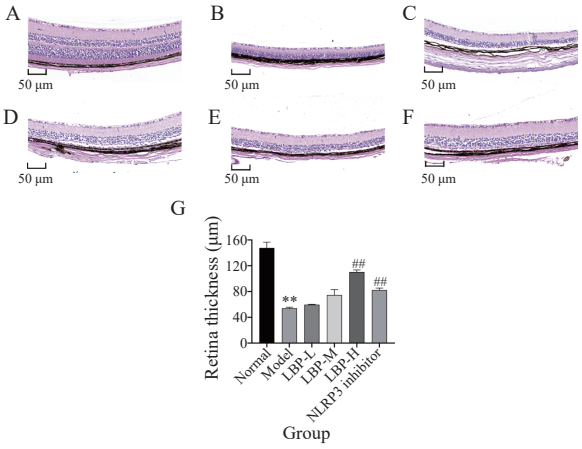

Figure 7 Morphological features of the retina detected by HE staining

A - F, ERG responses in the normal, model, LBP-L, LBP-M, LBP-H, and NLRP3 inhibitor groups, respectively. G, ONL thicknesses in each group. Data were expressed as mean ± SD. $^{**}P$ < 0.01, compared with the normal group. $^{\#\#}P$ < 0.01, compared with the model group.

3.8 Effects of LBP on IL-1β and TNF-α in the retina of Rd10

The expression levels of IL-1β and TNF-α in the retina of Rd10 mice exhibited a notable increase when compared with the normal group (P < 0.01). Remarkably, the administration of the high dose of LBP led to a significant decrease (P < 0.01) in the expressions of both IL-1β and TNF-α in the retina of Rd10 mice, and the extent of this reduction was dose-dependent on LBP (Figure 8).

3.9 Effects of LBP on the expression of proteins in the retina of Rd10 mice

WB was carried out to evaluate the effects of LBP on the protein levels of NF-κB, p-NF-κB, NLRP3, caspase-3, and the rate of Bax/Bcl-2 in all groups. The protein levels of NF-κB, p-NF-κB, and NLRP3 starkly increased in Rd10 mice within the model group in comparison to the normal group mice (P < 0.01). In contrast, the protein levels of NF-κB (P < 0.05), caspase-3, NLRP3, p-NF-κB, and the rate of Bax/Bcl-2 were markedly reduced in the LBP-H group in comparison to the model group (P < 0.01). These compelling findings suggested that LBP effectively inhibited the expressions of NF-κB, p-NF-κB, NLRP3, caspase-3, and decrease the rate of Bax/Bcl-2 in the retina of Rd10 mice (Figure 9).

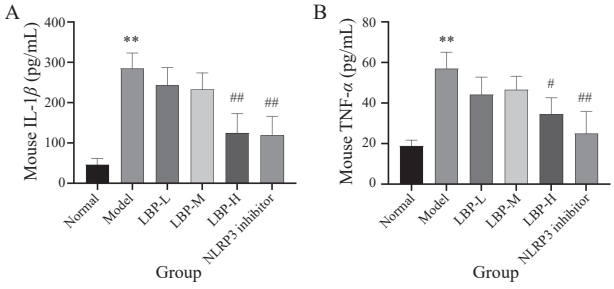

Figure 8 The expression levels of IL-1β and TNF-α in the retina of Rd10 mice by ELISA

A, the expression level of IL-1β. B, the expression level of TNF-α. Data were expressed as mean ± SD. $^{**}P$ < 0.01, compared with the normal group. $^{\#}P$ < 0.05 and $^{\#\#}P$ < 0.01, compared with the model group.

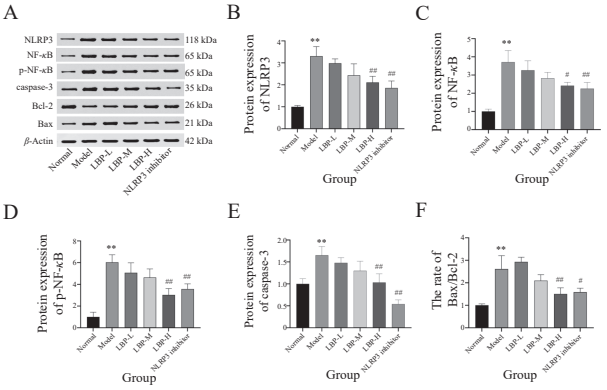

Figure 9 The expression levels of key proteins in NF-κB/NLRP3 pathway and apoptosis markers in different groups

A, the protein bands of NLRP3, NF-κB, p-NF-κB, caspase-3, Bcl-2, and Bax in mice. B - F, the quantitative evaluation of the proteins of NLRP3, NF-κB, p-NF-κB, caspase-3, and the rate of Bax/Bcl-2 in mice, respectively. Data were expressed as mean ± SD. $^{**}P$ < 0.01, compared with the normal group. $^{\#}P$ < 0.05 and $^{\#\#}P$ < 0.01, compared with the model group.

4 Discussion

RP is characterized by progressive degeneration and demise of photoreceptor cells [3]. Among the various forms of cell death studied in retinal degeneration, apoptosis has garnered the most attention [19, 20]. Photoreceptors, owing to their heightened metabolic rate and elevated oxygen consumption, are particularly vulnerable to oxidative stress [20]. Oxidative stress is a potential

contributor to the initiation of apoptosis in photoreceptors. anti-oxidant treatment demonstrated down-regulating effects on inflammatory markers and apoptotic events through modulation of the NF-κB pathway in Rd10 mice [21]. In this study, photoreceptors subjected to oxidative stress exhibited *in vivo* and *in vitro* activation of NF-κB, along with up-regulation of NLRP3, IL-1β, TNF-α, Bax, and caspase-3, accompanied by a simultaneous down-regulation of Bcl-2. Consistently, evaluations utilizing ERG and HE staining indicated that inflammation altered the structure of photoreceptor cells and impaired visual function when subjected to oxidative stress. Our study suggested that oxidative stress served as a trigger for the activation of NF-κB/NLRP3 pathways in photoreceptors, ultimately culminated in apoptotic events, both *in vivo* and *in vitro*. The levels of NF-κB/NLRP3 and apoptosis markers in the retina of Rd10 mice and 661W cells under oxidative stress were also analyzed. The results revealed that LBP intervention could inhibit the expression of these markers.

Inflammatory events are the primary factors believed to drive the progressive cellular deterioration observed in RP, potentially arising from both dys-regulated oxidant production and deficiencies in anti-oxidant capacity of RP [20]. The NF-κB/NLRP3 inflammasome pathway appears to play a pivotal role in photoreceptor loss and the subsequent risk of vision impairment in the presence of oxidative stress. The induction of NF-κB could lead to photoreceptor apoptosis via chronic inflammation in the retinas of the Rd10 mice [22]. The NF-κB-mediated transcriptional up-regulation of NLRP3 is important in the activation of inflammasome. A substantial increase in NLRP3 mRNA levels was observed within photoreceptors, and this increase was associated with the induction of cell apoptosis in patients suffering from retinal degeneration [23]. The induction of the NLRP3 inflammasome amplifies cytotoxicity, affecting neighboring cone photoreceptors in a P23H Rhodopsin model of retinal degeneration [24]. The activated NLRP3 inflammasome was reported to increase the levels of IL-1β and TNF-α [25, 26], which were crucial in the immune process. Therefore, the suppression of the two proteins could lead to immunosuppression. In inflammation-associated diseases, the inhibition of IL-1β and TNF-α could minimize cellular damages and provide positive clinical outcomes [25, 26]. In both *in vivo* and *in vitro* experiments, it was observed that NF-κB/NLRP3 inflammasome and apoptosis markers were higher in the model group compared with the normal group. Under oxidative stress conditions, the NF-κB/NLRP3 pathway was activated in Rd10 mice and 661W cells, the levels of inflammatory factors and cell apoptosis increased.

LBP from Gouqizi (*Lycium barbarum*) clearly exhibited anti-oxidant and anti-inflammatory effects, with active compounds mainly consisting of L-arabinose, D-fucose, D-glucose, D-galactose, D-rhamnose, and D-xylose [27-29]. Gouqizi (*Lycium barbarum*) has demonstrated the potential to enhance the activity of enzymes like glutathione peroxidase and superoxide dismutase, while concurrently reducing levels of malondialdehyde, all of which collectively contributed to a decrease in oxidative activities [30]. In addition, it was reported that the immunomodulatory effect of Gouqizi (*Lycium barbarum*) was primarily attributed to its polysaccharides content, and its immunomodulatory properties might have an effect on neurodegenerative processes in the central nerve system [28]. It was found that pre-treatment with LBP reduced the secretion of inflammatory molecules, such as TNF-α, IL-1β, and IL-6 by regulating NF-κB level [31]. LBP alone also was reported to have anti-apoptotic and anti-inflammatory effects by inhibiting hepatic caspase-3 activity and decreasing hepatic TNF-α levels in rats with CCl_4-induced liver fibrosis [32]. The administration of LBP by mice with liver injury was effective in protecting liver through attenuating NLRP3 and decreasing NF-κB activity, without the presence of any adverse effects [16]. Our previous study revealed that LBP inhibited H_2O_2-induced apoptosis and re-balanced autophagy in RPE cells via the microRNA-181/Bcl-2 pathway [5]. Furthermore, this study demonstrated that LBP treatment suppressed apoptosis in photoreceptors by inactivating NF-κB/NLRP3 inflammasome under oxidative stress, thus mitigating the loss of photoreceptors and improving the viability of cells in RP mice, suggesting LBP played a potential role in suppressing photoreceptor apoptotic events and improving retinal function.

To sum up, the study revealed that oxidative stress and inflammation could contribute to the loss of photoreceptors in RP mice. Morever, LBP treatment was able to prevent photoreceptor loss in RP mice by inhibiting NF-κB/NLRP3 pathway. Nonetheless, more research should be conducted to determine whether the inflammasome activation changes the type of cell death from apoptosis to pyroptosis and if LBP affects the pyroptosis.

5 Conclusion

This study speculated that LBP could improve the morphology and function of retina and protect photoreceptors from apoptosis by suppressing the NF-κB/NLRP3 pathway.

Fundings

National Natural Science Foundation of China (82274341), Scientific Research Project of Traditional Chinese Medicine of Hunan Province (B2023041), and Qihuang Scholars Support Project of PENG Qinghua, the Scientific Research Project of Hunan Provincial Department of Education (21B0391).

Competing interests

The authors declare no conflict of interest.

References

[1] LIMOLI PG, VINGOLO EM, LIMOLI C, et al. Anti-oxidant and biological properties of mesenchymal cells used for therapy in retinitis pigmentosa. Antioxidants, 2020, 9(10): 983.

[2] DIAS MF, JOO K, KEMP JA, et al. Molecular genetics and emerging therapies for retinitis pigmentosa: basic research and clinical perspectives. Progress in Retinal and Eye Research, 2018, 63: 107–131.

[3] NEWTON F, MEGAW R. Mechanisms of photoreceptor death in retinitis pigmentosa. Genes, 2020, 11(10): 1120.

[4] WANG J, LI ML, GENG ZY, et al. Role of oxidative stress in retinal disease and the early intervention strategies: a review. Oxidative Medicine and Cellular Longevity, 2022, 2022: 7836828.

[5] YANG YJ, WANG Y, DENG Y, et al. *Lycium barbarum* polysaccharides regulating miR-181/Bcl-2 decreased autophagy of retinal pigment epithelium with oxidative stress. Oxidative Medicine and Cellular Longevity, 2023, 2023: 1-18.

[6] CARMODY RJ, COTTER TG. Oxidative stress induces caspase-independent retinal apoptosis *in vitro*. Cell Death and Differentiation, 2000, 7(3): 282–291.

[7] FABIANI C, ZULUETA A, BONEZZI F, et al. 2-Acetyl-5-tetrahydroxybutyl imidazole (THI) protects 661W cells against oxidative stress. Naunyn Schmiedebergs Archives of Pharmacology, 2017, 390(7): 741–751.

[8] SCHWARTZ SG, WANG X, CHAVIS P, et al. Vitamin A and fish oils for preventing the progression of retinitis pigmentosa. The Cochrane Database of Systematic Reviews, 2020, 6(6): CD008428.

[9] GHASEMI H, GHAZANFARI T, YARAEE R, et al. Roles of IL-8 in ocular inflammations: a review. Ocular Immunology and Inflammation, 2011, 19(6): 401–412.

[10] MURAKAMI Y, ISHIKAWA K, NAKAO S, et al. Innate immune response in retinal homeostasis and inflammatory disorders. Progress in Retinal and Eye Research, 2020, 74: 100778.

[11] MURAKAMI Y, NAKABEPPU Y, SONODA KH. Oxidative stress and microglial response in retinitis pigmentosa. International Journal of Molecular Sciences, 2020, 21(19): 7170.

[12] KAARNIRANTA K, BLASIAK J, LITON P, et al. Autophagy in age-related macular degeneration. Autophagy, 2023, 19(2): 388–400.

[13] HOLLINGSWORTH TJ, HUBBARD MG, LEVI HJ, et al. Proinflammatory pathways are activated in the human Q344X rhodopsin knock-in mouse model of retinitis pigmentosa. Biomolecules, 2021, 11(8): 1163.

[14] LIU H, CUI B, ZHANG Z. Mechanism of glycometabolism regulation by bioactive compounds from the fruits of *Lycium barbarum*: a review. Food Research International, 2022, 159: 111408.

[15] TIAN XJ, LIANG TS, LIU YL, et al. Extraction, structural characterization, and biological functions of *Lycium barbarum* polysaccharides: a review. Biomolecules, 2019, 9(9): 389.

[16] XIAO J, WANG F, LIONG EC, et al. *Lycium barbarum* polysaccharides improve hepatic injury through NF kappa-B and NLRP3/6 pathways in a methionine choline deficient diet steatohepatitis mouse model. International Journal of Biological Macromolecules, 2018, 120(Pta 2): 1480–1489.

[17] ZHOU J, WANG FX, JIA LN, et al. 2,4-Dichlorophenoxyacetic acid induces ROS activation in NLRP3 inflammatory body-induced autophagy disorder in microglia and the protective effect of *Lycium barbarum* polysaccharide. Environmental Toxicology, 2022, 37(5): 1136–1151.

[18] LIU H, LIU LL, CHEN J, et al. Muscone with attenuation of neuroinflammation and oxidative stress exerts antidepressant-like effect in mouse model of chronic restraint stress. Oxidative Medicine and Cellular Longevity, 2022, 2022: 3322535.

[19] COMITATO A, SANGES D, ROSSI A, et al. Activation of Bax in three models of retinitis pigmentosa. Investigative Ophthalmology & Visual Science, 2014, 55(6): 3555–3562.

[20] KAUR G, SINGH NK. The role of inflammation in retinal neurodegeneration and degenerative diseases. International Journal of Molecular Sciences, 2021, 23(1): 386.

[21] CHEN Y, YANG M, WANG ZJ. (Z)-7,4'-Dimethoxy-6-hydroxyaurone-4-O-β-glucopyranoside mitigates retinal degeneration in Rd10 mouse model through inhibiting oxidative stress and inflammatory responses. Cutaneous and Ocular Toxicology, 2020, 39(1): 36–42.

[22] LOTFI P, TSE DY, DI RONZA A, et al. Trehalose reduces retinal degeneration, neuroinflammation and storage burden caused by a lysosomal hydrolase deficiency. Autophagy, 2018, 14(8): 1419–1434.

[23] BRANDSTETTER C, PATT J, HOLZ FG, et al. Inflammasome priming increases retinal pigment epithelial cell susceptibility to lipofuscin phototoxicity by changing the cell death mechanism from apoptosis to pyroptosis. The Journal of Photochemistry and Photobiology B, 2016, 161: 177–183.

[24] VIRINGIPURAMPEER IA, METCALFE AL, BASHAR AE, et al. NLRP3 inflammasome activation drives bystander cone photoreceptor cell death in a P23H rhodopsin model of retinal degeneration. Human Molecular Genetics, 2016, 25(8): 1501–1516.

[25] WU N, WU D, ZHAO M, et al. Clinical benefits of TNF-α inhibitors in Chinese adult patients with NLRP3-associated autoinflammatory disease. Journal of Internal Medicine, 2021, 290(4): 878–885.

[26] AJOOLABADY A, NATTEL S, LIP GYH, et al. Inflammasome signaling in atrial fibrillation: JACC State-of-the-Art Review. Journal of the American College of Cardiology, 2022, 79(23): 2349–2366.

[27] FAKHFAKH J, ATHMOUNI K, MALLEK-FAKHFAKH H, et al. Polysaccharide from *Lycium arabicum*: structural features, *in vitro* antioxidant activities and protective effect against oxidative damage in human erythrocytes. Chemistry & Biodiversity, 2020, 17(12): e2000614.

[28] CHANG RCC, SO KF. Use of anti-aging herbal medicine, *Lycium barbarum*, against aging-associated diseases. What do we know so far? Cellular and Molecular Neurobiology, 2008, 28(5): 643–652.

[29] TANG HL, CHEN C, WANG SK, et al. Biochemical analysis and hypoglycemic activity of a polysaccharide isolated from the fruit of *Lycium barbarum* L.. International Journal of Biological Macromolecules, 2015, 77: 235–242.

[30] OU C, JIANG PF, TIAN Y, et al. Fructus Lycii and *Salvia miltiorrhiza* Bunge extract alleviate retinitis pigmentosa through

Nrf2/HO-1 signaling pathway. Journal of Ethnopharmacology, 2021, 273: 113993.

[31] LIU ZC, YU WW, ZHOU HC, et al. *Lycium barbarum* polysaccharides ameliorate LPS-induced inflammation of RAW264.7 cells and modify the behavioral score of peritonitis mice. Journal of Food Biochemistry, 2021, 45(10): e13889.

[32] GAN F, LIU Q, LIU Y, et al. *Lycium barbarum* polysaccharides improve CCl_4 induced liver fibrosis, inflammatory response and TLRs/NF-κB signaling pathway expression in Wistar rats. Life Sciences, 2018, 192: 205–212.

枸杞多糖通过抑制 NF-κB/NLRP3 通路减少视网膜色素变性小鼠感光细胞凋亡

王英[a], 邓颖[b], 逯晶[c,d], 彭俊[a,c], 周亚莎[a,b,c], 杨毅敬[c*], 彭清华[a*]

a. 湖南中医药大学附属第一医院眼科, 湖南 长沙 410007, 中国
b. 湖南中医药大学中医学院, 湖南 长沙 410208, 中国
c. 中医药防治眼科耳鼻喉疾病湖南省重点实验室, 湖南 长沙 410208, 中国
d. 湖南中医药大学医学院, 湖南 长沙 410208, 中国

【摘要】目的 探讨枸杞多糖可否通过抑制核因子激活的 B 细胞的 κ-轻链增强子/NOD 样受体热蛋白结构域相关蛋白 3(NF-κB/NLRP3)信号通路减少视网膜色素变性(RP)小鼠视网膜光感受器细胞的凋亡。**方法** (1)体外实验将小鼠视网膜神经节细胞(661W 细胞)分为正常组、模型组、枸杞多糖低剂量组(40 mg/L)、中剂量组(80 mg/L)、高剂量组(160 mg/L)和阳性药物对照组(NLRP3 抑制剂, 160 mg/L); 分别用 50、100、200 和 400 μmol/L 四种剂量的 H_2O_2 干预 661W 细胞, 选出最佳 H_2O_2 浓度(200 μmol/L)造模, 细胞计数试剂盒 CCK-8 测定细胞活力, 流式细胞仪检测细胞凋亡率, 免疫荧光检测 NLRP3 标志物的表达, 酶联免疫吸附试验(ELISA)和免疫印迹法(WB)检测细胞凋亡标志物的表达。(2)选用 C57/BL6 小鼠和 Rd10 小鼠进行体内实验, 分组为正常组、模型组、枸杞多糖低剂量组(0.08 g/d)、中剂量组(0.16 g/d)、高剂量组(0.32 g/d)和阳性药物对照组(NLRP3 抑制剂, 0.08 g/d), 其中正常组为 C57/BL6 小鼠, 其余组为 Rd10 小鼠, 每组 10 只, 相对应的药物连续灌胃 4 周, 通过视网膜电图、组织病理学检查和 WB 等方法观察 NF-κB/NLRP3 通路及细胞凋亡标志物的表达, 评估枸杞多糖对视网膜光感受器细胞凋亡的影响。**结果** (1)体外实验中, 与正常组相比, 模型组 661W 细胞凋亡率明显增加($P < 0.01$), 且 NF-κB/NLRP 通路关键蛋白 NLRP3、NF-κB、p-NF-κB 和促凋亡蛋白 caspase-3 的表达水平上调($P < 0.01$), Bax/Bcl-2 的比值增大($P < 0.01$), 白细胞介素(IL)-1β 和肿瘤坏死因子(TNF)-α 的浓度显著升高($P < 0.01$)。与模型组相比, 高剂量的枸杞多糖降低了 661W 细胞的凋亡率($P < 0.01$), 下调了 NF-κB/NLRP3 通路关键蛋白 NF-κB、NLRP3、p-NF-κB 和 caspase-3 的表达($P < 0.01$), 减小了 Bax/Bcl-2 的比值($P < 0.01$), 降低了 IL-1β 和 TNF-α 的浓度($P < 0.01$)。(2)体内实验中, 高剂量的枸杞多糖显著增加了 Rd10 小鼠外核层(ONL)厚度的形态变化以及 a 波和 b 波振幅的功能变化($P < 0.01$), 下调了 NF-κB($P < 0.05$)、NLRP3、p-NF-κB 和 caspase-3 的表达水平($P < 0.01$), 减小了 Bax/Bcl-2 的比值($P < 0.01$), 降低了 IL-1β ($P < 0.01$)和 TNF-α($P < 0.05$)的浓度。**结论** 枸杞多糖可能通过抑制 NF-κB/NLRP3 通路改善视网膜形态和功能, 保护光感受器免受细胞凋亡的影响。

【关键词】视网膜色素变性; 枸杞多糖; 细胞凋亡; NF-κB/NLRP3 通路; 氧化应激